Available online at www.sciencedirect.com
SCIENCE DIRECT®
Polymer 44 (2003) 7335–7344
polymer
www.elsevier.com/locate/polymer

Synthetic hydrogels 2. Polymerization induced phase separation in acrylamide systems

Alan Y. Kwok, Emma L. Prime, Greg G. Qiao, David H. Solomon*

Polymer Science Group, Department of Chemical and Biomolecular Engineering, The University of Melbourne, Victoria, 3010, Australia

Received 26 May 2003; received in revised form 18 August 2003; accepted 4 September 2003

Abstract

Acrylamide hydrogels were synthesized in the presence of various non-solvents for linear polyacrylamide to examine phase separation during polymerization. The process was found to be dependent upon the segmental volume, the chemical structure, and the concentration of the non-solvent. The concept of conversion-phase diagram for linear polymer is introduced and used qualitatively to understand polymerization induced phase separation (PIPS), and to predict the onset of PIPS during hydrogel synthesis.

Keywords: Acrylamide hydrogel; Solvent; Phase separation

1. Introduction

Polymerization induced phase separation (PIPS) is a process in which an initially homogeneous solution of monomer and solvent becomes phase separated during the course of its polymerization. In hydrogel synthesis, PIPS can be induced by a number of factors: continuous increase in the fraction of molecules with high molecular weight, the unfavourable interactions between the polymer and other species in the reaction mixture, or the elasticity of the resultant polymeric network [1,2]. Depending on the relative rates of the phase separation and the polymerization processes, PIPS can occur by the mechanism of nucleation-growth in the metastable region, or by spinodal decomposition in the multiphase coexisting region of the phase diagram [3,4].

PIPS is widely employed to prepare various polymeric materials, for example porous thermosetting polymers [5], macroporous materials for chromatography [6], and liquid crystal dispersed polymer films [7]. Recently, Righetti and his co-workers [8] have synthesized macroporous acrylamide hydrogels by the addition of hydrophilic polymers into the monomer mixtures. It was postulated that competition between the gelation process and the phase separation process is responsible for the formation of pores that are much larger than those obtained in the absence of the hydrophilic polymer.

In our first paper of this series [9], we investigated the effects of solvent on the synthesis of acrylamide hydrogel; in this paper, we present results relating to a number of systems where there is the possibility of PIPS. The concept of conversion-phase diagrams is first introduced and later used in a discussion on the influences of the polymerization medium on PIPS.

2. Materials and methods

2.1. Materials

Acrylamide (AAm) (electrophoresis grade, >99.9%) was obtained from ICN Biochemicals (Aurora, OH, USA). *N*,*N*′-methylenebisacrylamide (Bis) (99%), *N*,*N*,*N*′*N*′-tetramethylethylenediamine (TEMED) (>99.5%), ammonium persulfate (APS) (>99.5%), tri(ethylene glycol) (>99%), tri(propylene glycol) (>97%), poly(ethylene glycol) (PEG, MW 400, MW 4000), poly(propylene glycol) (PPG, MW 425), and 3-(trimethylsilyl)propionic-2,2,3,3-d_4 acid, sodium salt (TMSPA-Na) (99 + %)were purchased from Aldrich Fine Chemicals (Castle Hill, NSW, Australia). Polyacrylamide (pAAm, MW 1,500, MW 10,000, MW 5,000,000–6,000,000) was obtained from Polysciences Inc.

* Corresponding author. Tel.: +613-834-48200; fax: +613-834-44153.
E-mail address: davids@unimelb.edu.au (D.H. Solomon).

0032-3861/$ - see front matter © 2003 Elsevier Ltd. All rights reserved.
doi:10.1016/j.polymer.2003.09.026

(Warrington, PA, USA). All reagents, unless specified, were of analytical grade and were used without further purification while distilled water was used at all times.

2.2. Conversion-phase diagram

The conversion-phase diagrams of pAAm (MW 1,500, MW 10,000, MW 5,000,000–6,000,000) were obtained by weighing the components, mixing them together, and leaving the samples for equilibration at 30 °C for 4 h.

2.3. Preparation of monomer solutions

Two terms, introduced in part I of this series [9], were used in the preparation of monomer solutions: %M refers to the total concentration of monomer as a weight percentage; %X refers to the number of double bonds on the crosslinkers as a portion of the total number of double bonds on the monomers. Unless specified, all other concentrations are in weight percentages.

$$\%\mathrm{M} = \frac{\text{total mass of monomers (g)}}{\text{mass of reaction mixture (g)}} \times 100 \quad (1)$$

$$\%\mathrm{X} = \frac{\text{number of double bonds on crosslinkers (mol)}}{\text{total number of double bonds on monomers (mol)}} \times 100 \quad (2)$$

2.4. Preparation of acrylamide hydrogels

Monomer solution (10 g) was prepared by dissolving AAm and Bis in the appropriate amount of water and PEG-400 in disposable glass vials. The solution was then degassed by argon purging prior to addition of the initiator system (0.05 mol% initiator per double bond) composed of freshly made up 10% (v/v) TEMED and 10% (w/v) APS. The polymerization was allowed to proceed at room temperature overnight under an argon environment.

2.5. Turbidity measurements of acrylamide hydrogel

Monomer solution (10 g) was prepared by dissolving AAm and Bis in the appropriate amount of water and PEG (or PPG). The solution was then degassed by argon purging prior to addition of the initiator system composed of freshly made up 10% (w/v) APS and 10% (v/v) TEMED (0.05 mol% initiator per double bond). Two 3.75 ml samples were pipetted into disposable cuvettes ($10 \times 10 \times 45$ mm^3) and the polymerization was allowed to proceed at room temperature overnight under an argon environment.

Turbidity measurements of the resultant gels was made using UV–visible spectrophotometry. Distilled water was used for the baseline and the absorbance of each gel sample was recorded at 600 nm. The turbidity of the gel samples was determined by the following equation.

$$\text{Turbidity} = -\ln(10^{-A}) \quad (3)$$

when A = absorbance of sample.

2.6. ^{13}C NMR relaxation measurements

Monomer solution (2 g) was prepared by dissolving AAm and Bis in the appropriate amount of D_2O (10% TMSPA-Na, 0.2 g), water and PEG-400. The solution was then degassed by argon purging prior to addition of the initiator system composed of freshly made up 10% (w/v) APS and 10% (v/v) TEMED (0.05 mol% initiator per double bond). This mixture was immediately pipetted into a 5 mm NMR tube (0.38 mm wall thickness) and the polymerization was allowed to proceed at room temperature overnight under an argon environment.

^{13}C NMR spectra were obtained using a Varian Unity Plus 400 spectrometer operating at 100 MHz. Spin-lattice relaxation times (T_1) were measured by the inversion-recovery method at 25 °C. Recycled delays were set to 7 s ($>3T_1$), with delay times (τ) of 10, 50, 100, 200, 300, 400, 500, 600, 700, 800, and 1000 ms. The T_1 parameters were calculated by fitting the data to the following equation.

$$I(\tau) = I(\tau = 0)(1 - 2\exp(-\tau/T_1)) \quad (4)$$

when I is the intensity of the transformed peaks.

2.7. Real-time viscosity measurements of acrylamide polymerizations

Monomer solution (200 g) was prepared by dissolving AAm and Bis in the appropriate amount of water and PEG-400. The solution was then degassed by argon purging prior to addition of the initiator system composed of freshly made up 10% (w/v) APS and 10% (v/v) TEMED (0.05 mol% initiator per double bond). The viscosity of the reaction mixture was measured by a Brookfield® DV-II + viscometer (0.3 rpm, LV-3 spindle). The experiment was performed in a glove box with controlled oxygen levels ($<0.1\%$ O_2).

3. Results and discussion

In a simplified formation process of acrylamide hydrogel by the free radical co-polymerization of acrylamide (AAm) and a divinyl crosslinker, linear polymers are first formed in the solution during the fast propagation step, and later crosslinked with other molecules in close proximity by reaction through their pendent double bonds and additional monomer units [10]. This work therefore uses

conversion-phase diagrams of linear polyacrylamide (pAAm) as a means to visualize the process of PIPS during the synthesis of acrylamide hydrogel.

3.1. Conversion-phase diagrams of linear pAAm

The free radical polymerization of *x*% AAm into pAAm, in the presence of a solvent (S) and a non-solvent (N) for the polymer, can be described as a line of constant solvent concentration in a rectangular S-N-AAm/pAAm diagram. We call such a diagram a conversion-phase diagram; the line of constant solvent concentration, along which the monomer conversion increases from the bottom to the top of the diagram, is called a polymerization line. Fig. 1 shows a typical conversion-phase diagram of pAAm, which can be divided into two regions—a region of miscibility (at high S contents and low monomer conversions) to the left, and a region of immiscibility (at low S contents and high monomer conversions) to the right of the phase boundary. The total fraction of AAm and pAAm (*x*%) and the total fraction of S and N (100 − *x*%) are constant for every point in the diagram. Boots et al. [2] have proposed a similar type of conversion-phase diagram for a three-component (monomer, polymer and solvent) system.

Fig. 1 shows three lines (A, B and C) that represent AAm polymerizations at different ratios of S and N. Line A describes the polymerization of *x*% monomer in the presence of a low concentration of N (high concentration of S); line B, an intermediate concentration of N; line C, a high concentration of N.

Line A shows that despite the continuous increases in the fraction of polymer in the reaction mixture, PIPS cannot occur over the entire range of monomer conversion. Line B can be divided into a miscible and an immiscible segment; PIPS can occur at a critical monomer conversion, which is dependent upon the relative rates of the polymerization and the phase separation processes. Line C describes the polymerization in the presence of a large amount N; when compared to line B, PIPS can occur at a lower monomer conversion.

Fig. 2 shows a number of experimental conversion-phase diagrams of pAAm-10,000 at 30 °C; the solvent for the polymer is water; the non-solvent for the polymer is poly(ethylene glycol) (PEG-150, PEG-400, or PEG-4000), a hydrophilic polymer known to induce PIPS during the synthesis of acrylamide hydrogel [8]. It can be seen from the phase boundaries that increases in the molecular weight of PEG produced conversion-phase diagrams with significantly larger regions of immiscibility. If the average molecular weight and molecular weight distribution of the resultant polymers are assumed to be identical with the commercial pAAm sample, Fig. 2 actually describes the homo-polymerization of 20%M acrylamide into pAAm-10,000 at different ratios of water and PEG. It can be seen that phase separation can occur when the reaction mixtures contain more than ~63% PEG-150, more than ~31% PEG-400, or more than ~6% PEG-4000.

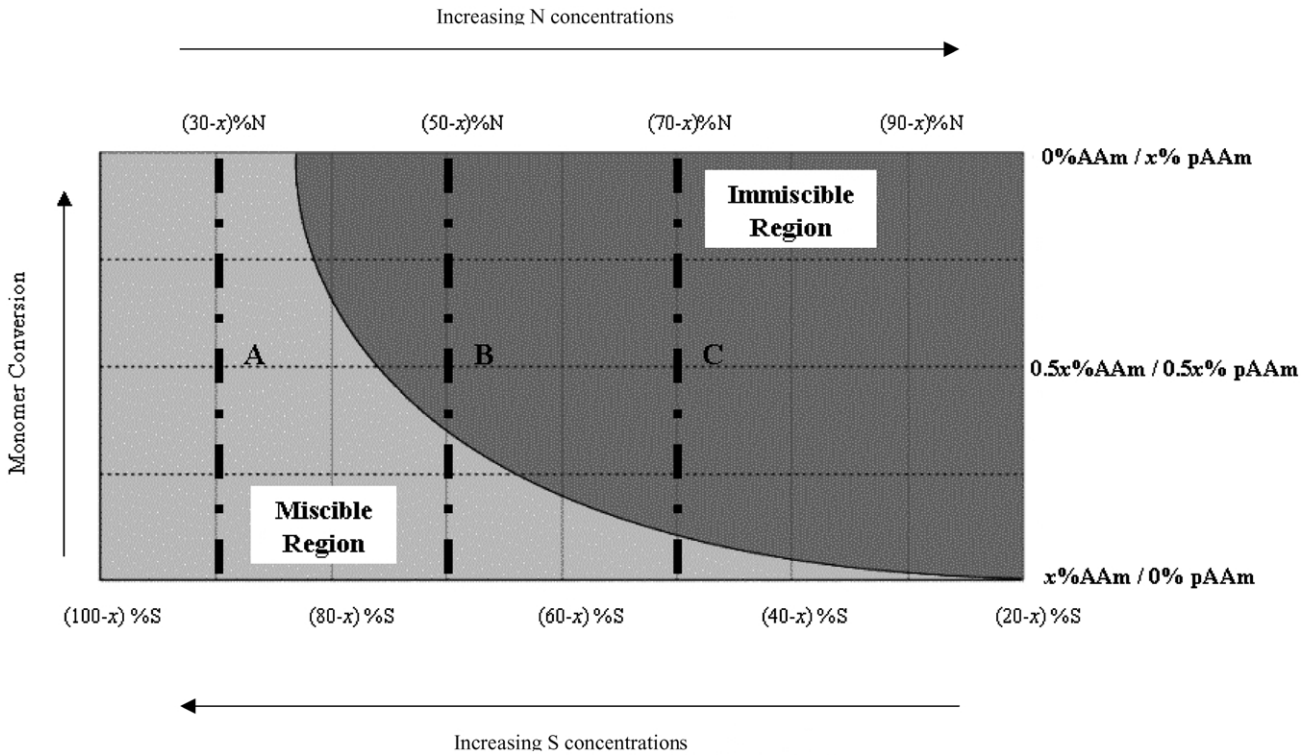

Fig. 1. A typical conversion-phase diagram which represents the free radical polymerization of *x*% AAm into pAAm in the presence of a solvent for the polymer (S) and a non-solvent for the polymer (N).

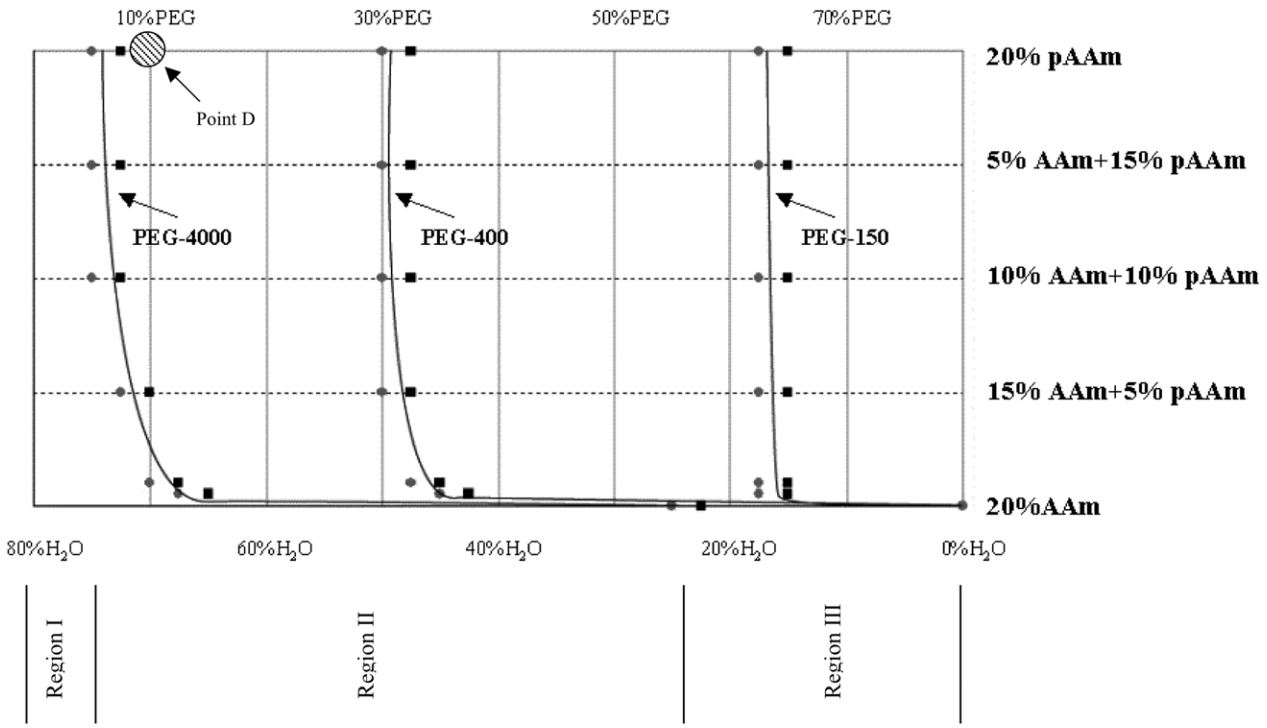

Fig. 2. Conversion-phase diagram of pAAm-10,000 in the presence of PEG-150, PEG-400 or PEG-4,000 at 30 °C. Immiscible samples are represented by dark coloured points (square); miscible samples are represented by lightly coloured points (circle).

Miscibility in a multi-component system is governed by its Gibbs free energy of mixing (ΔG_{mix}), which is a function of the enthalpies of mixing and the entropies of mixing between the various components in the mixture ($\Delta G_{mix} = \Delta H_{mix} - T\Delta S_{mix}$). Various phase diagrams—depending on polymer–polymer miscibility, polymer molecular weights, and solvent affinities of each polymer component—can appear for multi-component systems that contain two chemically different polymers [11]. The immiscible regions in Fig. 2, located at high concentrations of pAAm or PEG, suggest that the phase behaviour of the system is similar to that of a ternary system which contains an immiscible polymer pair dissolved in a common, good solvent (water). In our previous paper [9], NMR analysis of AAm in aqueous solutions of pAAm has shown that the amount of water required to solvate pAAm is less than that required to solvate AAm. In contrast to the ternary systems, the role of AAm in the conversion-phase diagram is therefore to shift the onset of phase separation towards higher water concentrations.

Because the enthalpy of mixing between two chemically different polymers is mostly positive, miscibility in systems that contain pAAm and low amounts of PEG can be attributed to the entropy gained by each component during the dissolution process. This theory is consistent with the observed relationship between miscibility and the chain length of PEG; increase in the molecular weight of PEG decreases the region of miscibility in the conversion-phase diagram because it decreases the entropy term in the ΔG_{mix} equation.

From Fig. 2, 20% AAm (represented by the line of 0% conversion) is soluble at all ratios of water and PEG in the presence of PEG-150 or PEG-400, but is insoluble in the presence of PEG-4000 when the water content of the mixtures is less than ~24%. The latter system can be divided into 3 regions: region I describes the polymerization of AAm in a medium which acts as a solvent for both the monomer and the polymer; region II, a medium which acts as a solvent for the monomer and the polymer at low monomer conversions, but as a solvent only for the monomer at higher monomer conversions; and region III, a medium which acts as a non-solvent for both the monomer and the polymer.

Fig. 3 shows conversion-phase diagrams of pAAm-1,500, pAAm-10,000, and pAAm-5,000,000-6,000,000 in the presence of PEG-400. Increases in the molecular weight of pAAm have similar effects to increases in the molecular weight of PEG; it produced conversion-phase diagrams with significantly larger regions of immiscibility. By comparing Figs. 2 and 3, it can be seen that increases in the molecular weight of PEG have a much greater effect on the miscibility of the system than increases in the molecular weight of pAAm. For example, if we consider a mixture with 70% water, 10% PEG and 20% pAAm (Point D on Figs. 2 and 3), the mixture remains miscible when the molecular weight of pAAm is increased from 10,000 to 5,000,000–6,000,000, but becomes immiscible when the molecular weight of PEG is increased from 400 to 4000. The different conformation of the two polymers in solution can explain this phenomenon-it is well accepted that PEG is highly compatible with water,

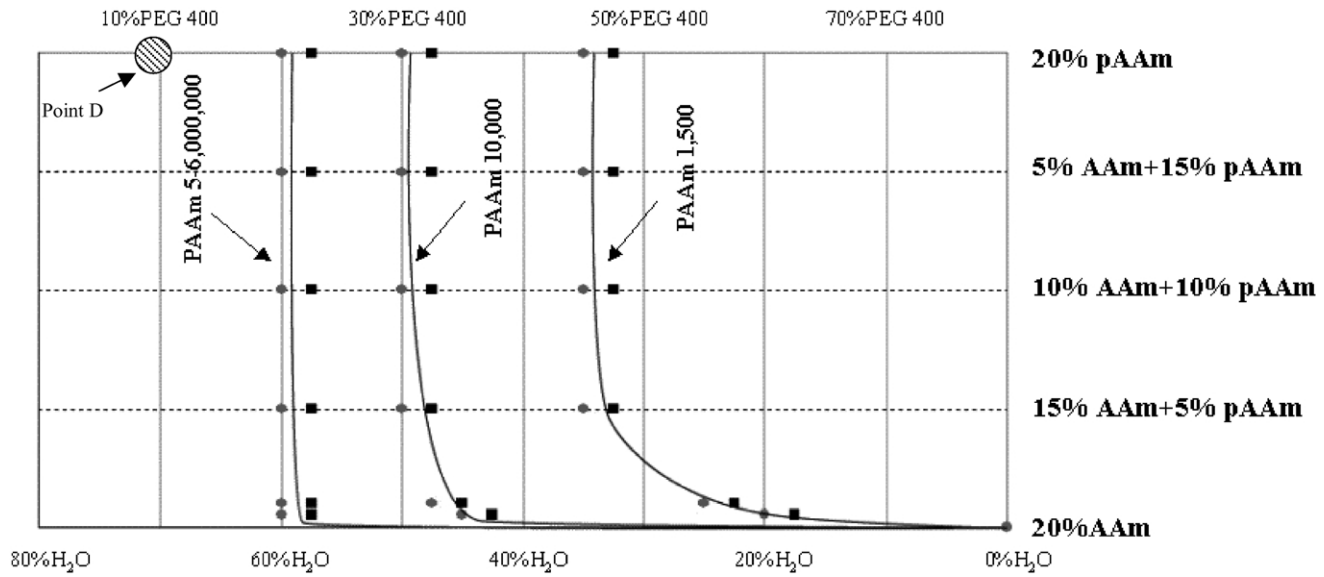

Fig. 3. Conversion-phase diagram of pAAm-1,500, pAAm-10,000, or pAAm-5,000,000–6,000,000 in the presence of PEG-400 at 30 °C. Immiscible samples are represented by dark coloured points (square); miscible samples are represented by lightly coloured points (circle).

and is capable of forming a rather rigid, bridged hydrogen-bond network in aqueous solutions [12,13]. PEG is therefore expected to have a greater influence on the phase behaviours of aqueous systems not only because the segmental volume of PEG in water is much greater than pAAm (a polymer with a more hydrophobic backbone [14]) but also because the solute–solute interactions between PEG molecules would further decrease their compatibility with pAAm.

3.2. Conversion-phase diagram and the gel formation process

In contrast to the homo-polymerization of mono-vinyl monomers, synthetic hydrogels are mostly obtained by the co-polymerization of mono-vinyl monomers and multi-vinyl monomers that act as crosslinkers. In this study, acrylamide hydrogels were synthesized by the use of *N*,*N*′-methylenebisacrylamide as crosslinker.

Turbidities of 20%M 2%X acrylamide hydrogels were measured as a function of the amount of PEG-400 in the polymerization mixture to monitor the extent of PIPS in the samples (Fig. 4). It was observed that turbidity of the gels begins to increase dramatically around 17.5% PEG-400, which corresponds to the appearance of visual opacity within the samples. The gels are clear at low PEG-400 concentrations, opaque at high PEG-400 concentrations, and slightly opalescent in an intermediate concentration range between the clear and the opaque region.

In order to confirm that the observed turbidity in the samples is not solely due to the pore size changes of the gels, NMR relaxational studies were performed to provide information about the network structure of the gels. Fig. 5 is a series of ^{13}C NMR spectra of a 20%M 2%X acrylamide hydrogel—synthesized in water—obtained by introducing various delay times in the inversion-recovery pulse sequence. The three peaks at 38 (peak a), at 45 (peak b), and at 182 ppm (peak c) are assigned to the α- and β-carbons on the polymer backbone, and the carbonyl carbon of the amide groups, respectively. A non-linear least square fit of the data (to eq (4)) gave T_1 to be 240 ms at the α-carbons, 130 ms at the β-carbons, and 1280 ms at the carbonyl carbons. It is well accepted that for diamagnetic systems, the most important mechanism for T_1 relaxation is the direct space interaction of two nuclear dipoles [15]; therefore, ^{13}C nuclei in natural abundance must usually rely on the presence of nearby protons to promote relaxation [16]. This can explain the fact that the carbonyl amide carbons, which are most distant from protons, have the longest T_1, while the β-carbons have the shortest T_1 because of the relatively large number of protons in its proximity.

Table 1 compares the T_1 values for the three carbon groups of acrylamide hydrogels which were synthesized in the presence of various amount of PEG-400. It can be seen that the T_1s are nearly constant at low concentrations of PEG-400; significant increases in T_1s are observed at 17.5% PEG-400 for the α- and β-carbons, and 22.5% PEG-400 for

Table 1
^{13}C T_1 (25 °C, 100 MHz) for 20%M 2%X acrylamide hydrogels synthesized in the presence of various amount of PEG-400

PEG-400 concentrations (%)	T_1(α-carbon) (ms)	T_1(β-carbon) (ms)	T_1(carbonyl) (ms)
0	240 ± 10	130 ± 5	1275 ± 20
2.5	240 ± 10	125 ± 5	1330 ± 20
7.5	240 ± 10	135 ± 5	1350 ± 20
12.5	261 ± 10	140 ± 5	1400 ± 20
17.5	280 ± 10	160 ± 10	1400 ± 50
22.5	340 ± 20	180 ± 5	1730 ± 50
27.5	420 ± 25	230 ± 10	2185 ± 55

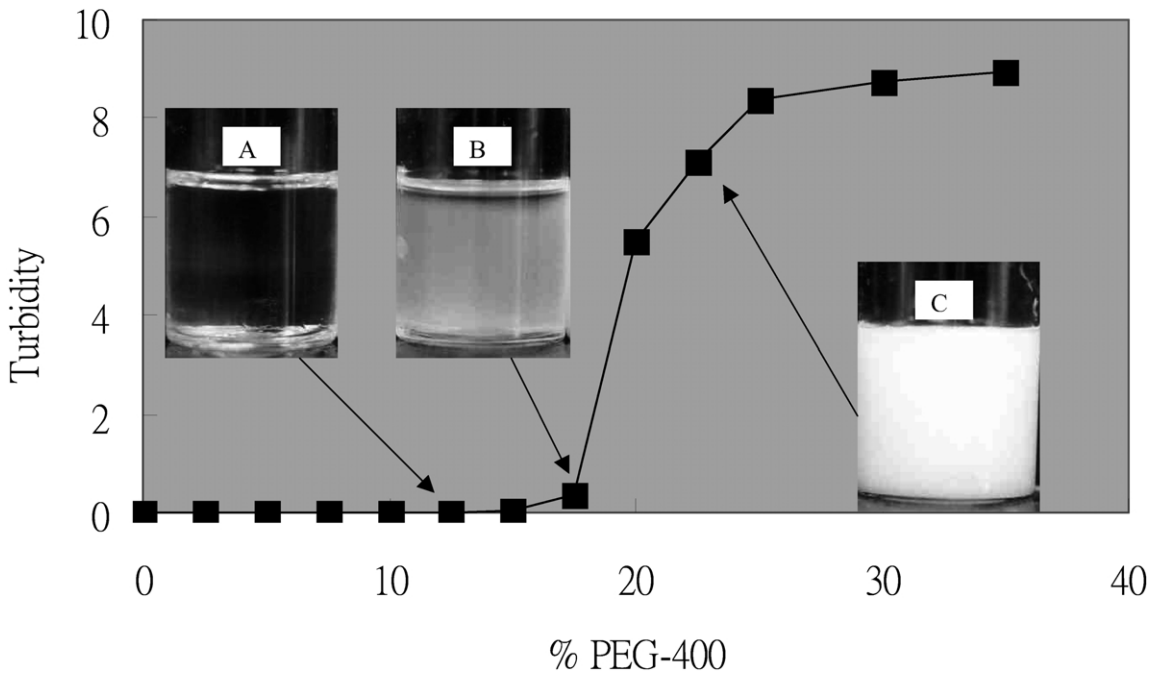

Fig. 4. Turbidity measurements of 20%M 2%X acrylamide hydrogels synthesized in the presence of various amounts of PEG-400. Gel A was synthesized in the presence of 12.5% PEG-400; Gel B, 17.5% PEG-400; Gel C, 22.5% PEG-400.

the carbonyl carbons. The observed results are consistent with our turbidity studies, and the expected reduction in segmental mobility of pAAm caused by precipitation during the phase separation process. The different critical PEG-400 concentrations for the onset of increases in T_1 at different carbon groups could be attributed to the relatively higher segmental mobility of the amide side chains compared with the secondary β-carbons and tertiary α-carbons on the polymer backbone.

From Figs. 3 and 4, it can be seen that the phase behaviour of 20%M 2%X acrylamide hydrogels is similar to that of linear pAAm-5,000,000–6,000,000; phase separations

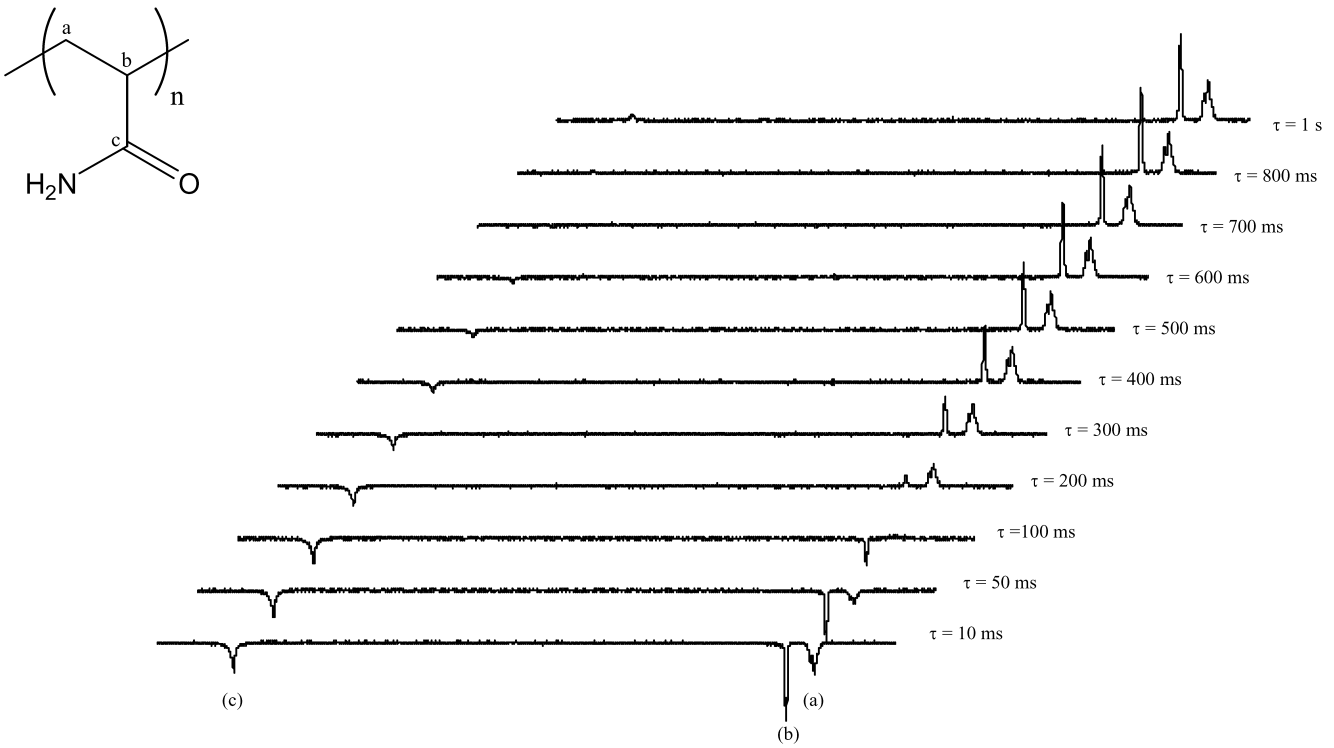

Fig. 5. ^{13}C NMR stack spectra of 20%M 2%X acrylamide hydrogel (synthesized in water) measured at 25 °C, 100 MHz.

of both systems were observed to occur at similar PEG concentrations. This observation is interesting because the definition of a gel—a network with infinite molecular weight which reaches the macroscopic dimensions of the sample itself [17]—implies that polymers with very high molecular weight are produced in the reaction mixture prior to the formation of a gel network. Although such polymers are branched (instead of linear), their polymer-N compatibility would be significantly less than that for linear polymers with finite molecular weight.

In order to investigate this phenomenon further, 20%M acrylamide hydrogels with different amounts of crosslinker were prepared in the presence of 0, 15, or 17.5% PEG-400. Turbidity measurements of the gels (Table 2) demonstrate that the onset of PIPS is dependent upon the crosslinker concentration—the turbidity of the gels increases with increasing crosslinker content. These results suggest that the miscibility of gel networks is not solely dependent upon the final molecular weight of the polymers. A possible explanation for this phenomenon can be obtained if we relate the concept of frozen concentration fluctuation—the process in which the dynamic concentration fluctuations of pre-gel polymer solutions are frozen in the final network structure upon the onset of the gelation process [18]—to the development of average molecular weight of polymers in the solutions.

In the pre-gel regime of the polymerization process—if we assume auto-acceleration in the polymerization rate is absent, and that the initiator efficiency is constant throughout the course of the polymerisation—increases in the molecular weight of polymers in the mixture can be attributed to crosslinking reactions between primary polymer molecules (the term, primary polymer molecule, describes the imaginary linear polymer which would exist if all the crosslinks connected to it were severed [17,19]). In this study, the theoretical development of average molecular weight in this regime was calculated according to the Macosko–Miller gelation theory, which is based on the recursive nature of the branching process and an elementary law of conditional expectation [20]. Although this theory retains the three simplifying assumptions of the classical gelation theory from Flory [21], we used it (in calculations of the polymerization lines in Fig. 6) to understand qualitatively the relationship between average molecular weight and monomer conversion at different crosslinker concentrations.

Table 2
Turbidity measurements of 20%M acrylamide hydrogels synthesized in the presence of 0, 15, or 17.5% PEG-400 at various %X

	Turbidity (%X)				
PEG-400 concentrations (%)	0	1	2	3	4
0	0.01	0.06	0.08	0.06	0.07
15	0.02	0.01	0.06	0.42	3.03
17.5	0.01	0.07	0.32	3.36	7.19

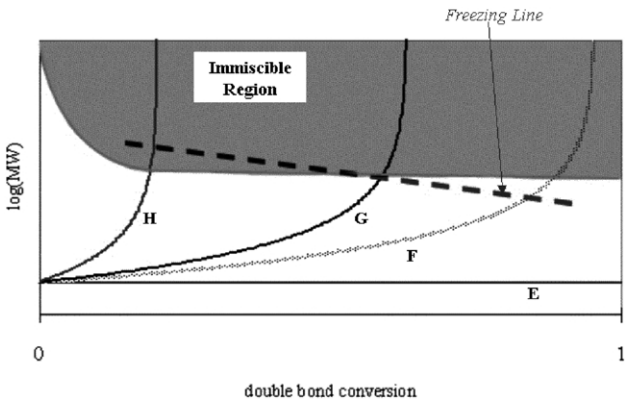

Fig. 6. Schematic diagram of the formation process of 20%M acrylamide hydrogels in the presence of a fixed concentrations of S and N. The polymerization lines were calculated according to Eq. (77–79) in [18], $q = 0.99$, $\%X(E) = 0$, $\%X(F) = 2$, $\%X(G) = 3$, and $\%X(H) = 10$.

Fig. 6 is a schematic diagram which represents the formation process of 20%M acrylamide hydrogels in the presence of fixed concentrations of S and N. Based on results from our conversion-phase diagrams, the system shows a region of immiscibility when a significant amount of pAAm with high molecular weight is present. Four polymerization lines are shown in the diagram: line E represents the homo-polymerization of AAm, during which it is assumed that the average molecular weight of the polymer remains constant at all monomer conversions. Line F, G and H represent crosslinking polymerizations of AAm at different concentrations of crosslinker ($\%X(F) < \%X(G) \ll \%X(H)$). The effective molecular weight of these polymer mixtures increases with increasing monomer conversion; the rate of increase in molecular weight is faster for systems with higher amounts of crosslinker.

We suggest C_F, the monomer conversion at which the 'freezing' of dynamic concentration fluctuations occurs, is reached when the viscosity of the mixture reaches a specific level at which the mobility of polymer chains in the mixture becomes negligible. C_F, like viscosity of polymer solutions, is a function of both the molecular weight and the concentration of polymers in the mixture. In contrast to the theoretical gel point, at which the average molecular weight of polymers is infinite [10], the average molecular weight of polymers at C_F is expected to decrease upon increasing C_F because the capacity of a polymer to enhance the solution viscosity increases with increasing molecular weight. The 'freezing line' in Fig. 6, simply assumed to be linear in this study, illustrates the above relationship between C_F and monomer conversion.

The properties of hydrogels in Fig. 6 are dependent on the location of their C_F in the phase diagram. For example, polymerization mixtures with a low amount of crosslinker (e.g. line F) can reach C_F well before the phase boundary;

therefore, the resultant gels are clear and have a relatively uniform network because the polymer mixture was 'frozen' in its miscible state before phase separation could occur. As the crosslinker concentration of the mixture increases, it becomes possible for C_F to be located at a position that is near to the phase boundary (e.g. line G). The resultant gels from these systems are slightly opalescent and more inhomogeneous because at C_F, although the average molecular weight of the polymers is below the phase separation threshold, the larger polymers included in the polydispersed mixture can undergo phase separation. The freezing process will permanently embed the resultant precipitated polymers in the gel network; therefore, the nearer C_F is to the phase boundary, the more opalescent (a measure of structural inhomogeneities) are the resultant hydrogels. When the crosslinker concentration of the mixture is further increased such that C_F is in the immiscible region of the phase diagram (e.g line H), phase separation would occur before the freezing of the mixture. This results in the formation of a dispersion of precipitated polymers in the liquid phase [22]; products from these systems are highly opaque polymer masses that can be used in various applications, depending on the extent of phase separation and the extent of crosslinking between the precipitated polymers [6].

In order to support the above theory, experimental data (Fig. 7) was obtained from real-time viscosity monitoring of the polymerization of acrylamide solutions with 17.5% PEG-400. It can be seen that the viscosity of the reaction mixtures remains constant over a certain time period, then increases quite markedly up to 400,000 cp (the upper detection limit of the viscometer). The length of the time period and the rate at which the viscosity increases were observed to be dependent upon the crosslinker content of the reaction mixture.

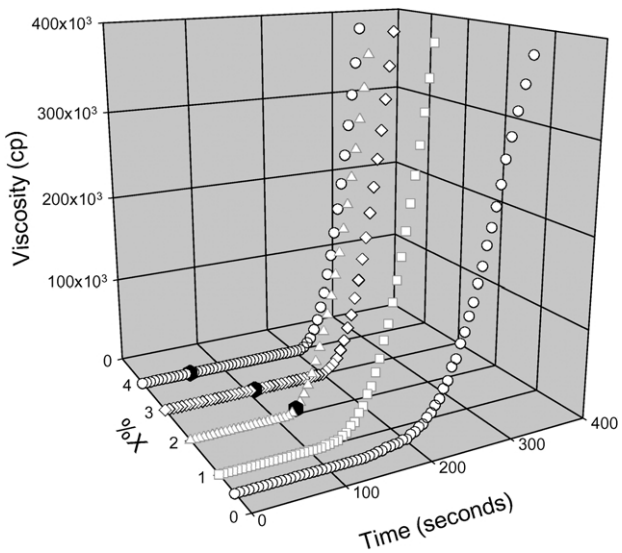

Fig. 7. Real-time viscosity measurements of the polymerization of 20%M acrylamide solutions, in the presence of 17.5% PEG-400, at various %X. Times at which phase separation was observed in the samples are represented by dark coloured points (circle).

In the absence of PIPS (at 1%X and 0.5%X), the increase in viscosity at higher %X of the reaction mixture was observed to occur earlier and more rapidly than that at lower %X. This phenomenon can be attributed to the increase in the probability of intermolecular crosslinking between polymer molecules. The resultant hydrogels from these systems are clear because the reaction mixture is described as being 'frozen' prior to phase separation. As the crosslinker content of the reaction mixture increases (i.e. $\geq$2%X), PIPS becomes possible because of the appearance of polymers with very high molecular weight—which are able to precipitate prior to the formation of a gel network—in the mixture. At 2%X, the onset of PIPS was observed to coincide with the increase in viscosity and the resultant gel is slightly opalescent because the monomer conversion for phase separation is close to C_F. At 3%X and 4%X, phase separation was observed prior to the increase in viscosity and highly opaque polymers are formed because PIPS occurs prior to the onset of gelation.

It is interesting to note that at 3%X and 4%X, the occurrence of PIPS was observed to delay the onset of viscosity increase of the reaction mixture. This phenomenon can be attributed to the fact that the viscosity of a solution of precipitated polymers is generally lower than that of a solution of solvated polymers, and the crosslinking efficiency between precipitated pAAms is also reduced.

3.3. Effect of N on PIPS

In addition to the ratio between N and S, the phase behaviour of a polymer solution is also dependent upon the segmental volume and the chemical structure of N. If again we consider the schematic diagram that represents the formation process of 20%M acrylamide hydrogels (Fig. 6), the region of immiscibility will increase as the N/S ratio increases, or as the N-pAAm compatibility decreases. It follows that the critical N concentration for the onset of PIPS is lower for systems that have higher ΔG_{mix}.

Results from our conversion-phase diagrams of pAAm indicate that miscibility in pAAm–PEG systems decreases with increasing chain length of PEG; therefore, the critical PEG concentration for the onset of PIPS in acrylamide hydrogels is expected to decrease with increasing molecular weight of PEG. Turbidity measurements of 20%M 2%X acrylamide hydrogels synthesized in different concentrations of PEG-150, PEG-400 or PEG-4000 (Fig. 8) support this prediction, and are consistent with results obtained by Righetti [23] on hydrogels synthesized in the presence of PEGs that have higher molecular weight than those used in our systems.

The importance of the chemical structure of N is demonstrated in Fig. 9 when PEG in the conversion-phase diagrams of pAAm is replaced with poly(propylene glycols) (PPG) that have similar molecular weights to their PEG

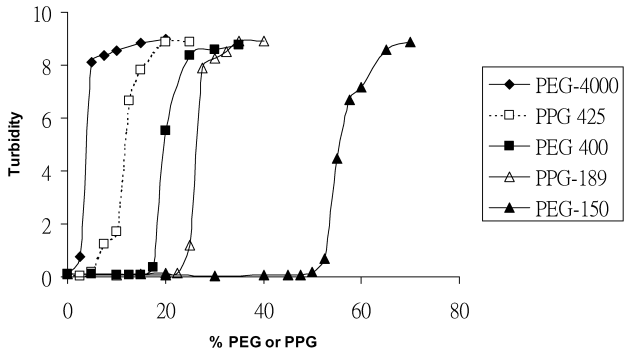

Fig. 8. Turbidity measurements of 20%M 2%X acrylamide hydrogels synthesized in the presence of various amounts of PEG-150, PEG-400, PEG-4000, PPG-189, or PPG-425.

analogues. It can be seen that the region of miscibility in PPG systems is significantly smaller than that in PEG systems. For example, PIPS can occur during the polymerization of 20%M AAm into pAAm 10,000 when the monomer mixtures contain more than ~16% PPG-425 or more than ~31% PEG-400, and more than ~31% PPG-189 or more than ~64% PEG-150.

Based on viscosity measurements of complexed aqueous solutions of pAAm and PEG, Dan et al. [24] suggested the existence of weak hydrogen bonding between the amide group of pAAm and the ether group of PEG. The methyl substituent on the PPG repeating unit produces considerable steric hindrance to bond rotation and can significantly limit the available space for hydrogen bonding to take place with the ether oxygen [25,26]; in contrast to PEG, the reduced miscibility in PPG systems can therefore be attributed to the larger mixing enthalpy of these mixtures.

Turbidity measurements of 20%M 2%X acrylamide hydrogels synthesized in different concentrations of PPG-425 or PEG-400, and PPG-189 or PEG-150 again agree with observations made in conversion-phase diagrams of pAAm. It can be seen in Fig. 8 that PIPS can be induced in hydrogel synthesis by a much lower concentrations of PPG when compared with PEG.

4. Conclusion

In this work we have introduced the concept of conversion-phase diagram and used such diagrams of linear pAAm to understand PIPS in the synthesis of acrylamide hydrogels. PIPS was observed during hydrogel synthesis in the presence of a non-solvent for pAAm; the different degrees of opaqueness of the resultant hydrogels were explained by a discussion on the concept of frozen concentration fluctuation and the development of average molecular weight in the pre-gel solution.

Conversion-phase diagrams of linear pAAm and turbidity measurements of acrylamide hydrogels in the presence of various non-solvents were used to demonstrate the relationship between the onset of PIPS, the segmental volume or chemical structure of the non-solvent. It was found that PIPS is promoted as the segmental volume of the non-solvent increases, or as the non-solvent-pAAm compatibility decreases.

It must be pointed out that as discussed in our previous paper [9], solvent variation in the synthesis of acrylamide hydrogel can also influence the chain lengths of the primary polymer molecules produced during the polymerization. Moreover, phase separation can also occur beyond the formation of a gel network because of the elasticity of the network. Discussion of the influences of these phenomena on PIPS does not form part of this investigation.

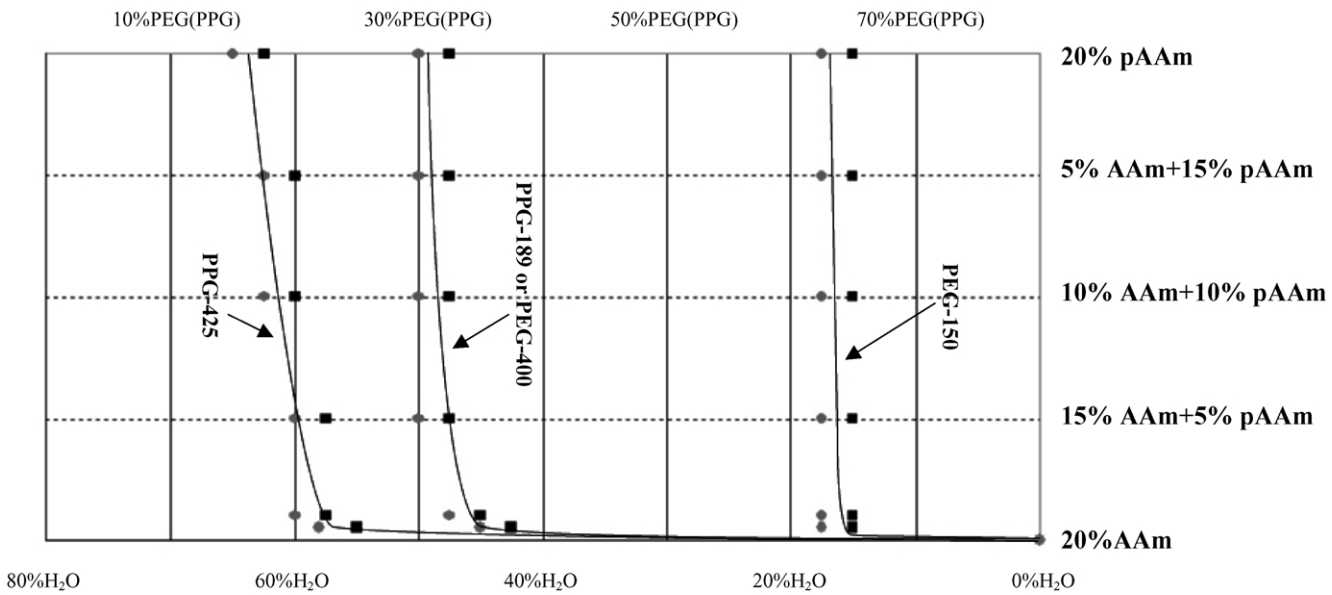

Fig. 9. Conversion-phase diagram of pAAm-10,000 in the presence of PPG-425, PPG-189, PEG-400 or PEG-150 at 30 °C. Immiscible samples are represented by dark coloured points (square); miscible samples are represented by lightly coloured points (circle).

Acknowledgements

We thank Prof. F. Separovic, Department of Chemistry, University of Melbourne, for technical assistance and valuable discussions on the NMR experiments. We would also like to acknowledge Gradipore Ltd, and the Australian Research Council for their financial support.

References

[1] Dušek KJ. Polym Sci Polym Symp 1967;16(3):1289–99.
[2] Boots HMJ, Kloosterboer JG, Serbutoviez C, Touwslager FJ. Macromolecules 1996;29(3):7683–9.
[3] Eliçabe GE, Larrondo HA, Williams RJJ. Macromolecules 1997; 30(21):6550–5.
[4] Eliçabe GE, Larrondo HA, Williams RJJ. Macromolecules 1998; 31(23):8173–82.
[5] Loera AG, Cara F, Dumon M, Pascault J. Macromolecules 2002; 35(16):6291–7.
[6] Okay O. Prog Polym Sci 2000;25(6):711–79.
[7] Nwabunma D, Chiu H, Kyu T. J Chem Phys 2000;113(15):6429–36.
[8] Asnaghi D, Giglio M, Bossi A, Righetti PG. J Mol Struct 1996;383(1–3):37–42.
[9] Kwok AY, Qiao GG, Solomon DH. Polymer 2003;44(20):6195–203.
[10] Stepto RFT. Non-linear polymerization, gelation and network formation, structure and properties. In: Stepto RFT, editor. Polymer networks. London: Blackie Academic and Professional; 1998. p. 14–63.
[11] Einaga Y. Prog Polym Sci 1994;19(1):1–28.
[12] Tasaki K. J Am Chem Soc 1996;118(35):8459–69.
[13] Vergara A, Paduano L, D'Errico G, Sartorio R. Phys Chem Chem Phys 1999;1(20):4875–9.
[14] Gromov VF, Bogachev YS, Bune YV, Zhuravleva IL, Teleshov EN. Eur Polym J 1991;27(6):505–8.
[15] King RW, Williams KR. J Chem Ed 1989;66(9):A213–9.
[16] Komoroski RA, Mandelkern L. Carbon-13 spin relaxation parameters of bulk synthetic polymers. In: Brame EG, editor. Applications of polymer spectroscopy. New York: Academic Press; 1978. p. 57–77.
[17] Flory PJ. Principles of polymer science. New York: Cornell University Press; 1953. Chapter IX.
[18] Matsuo ES, Orkisz M, Sun S, Li Y, Tanaka T. Macromolecules 1994; 27(23):6791–6.
[19] Tobita H, Hamielec AE. Polymer 1992;33(17):3647–57.
[20] Macosko CW, Miller DR. Macromolecules 1976;9(2):199–206.
[21] Flory PJ. J Am Chem Soc 1941;63:3083–90.
[22] Okay O. Polymer 1999;40(14):4117–29.
[23] Righetti PG. J Chromatogr A 1995;698(1 + 2):3–17.
[24] Dan Y, Chen S, Zhang Y, Xiang F. J Polym Sci, Part B: Polym Phys 2000;38(8):1069–77.
[25] Vachon C, Vasco M, Perrier M, Prud'homme J. Macromolecules 1993;26(15):4023–31.
[26] Panayiotou C, Sanchez IC. Macromolecules 1991;24(23):6231–7.